AD 400 574

Technical Note SSD-TDR-63-42

Menlo Park, California

IONIZATION IN AFTERBURNING ROCKET EXHAUSTS

CONRAD F. SCHADT
STANFORD RESEARCH INSTITUTE

QUARTERLY REPORT NO. 2, PART I
January 1963

Contract AF 04(694)-128
SRI Project PAU 4134-1

400574

Prepared for

HEADQUARTERS
SPACE SYSTEMS DIVISION
AIR FORCE SYSTEMS COMMAND
UNITED STATES AIR FORCE
Air Force Unit Post Office
Los Angeles 45, California

Technical Note SSD-TDR-63-42

IONIZATION IN AFTERBURNING ROCKET EXHAUSTS

Conrad F. Schadt
Stanford Research Institute

Quarterly Report No. 2 Part I
January, 1963

Contract AF 04(694)-128
SRI Project PAU 4134-1

Covering the period
1 September to 1 December 1962

Prepared for

HEADQUARTERS
SPACE SYSTEMS DIVISION
AIR FORCE SYSTEMS COMMAND
UNITED STATES AIR FORCE
Air Force Unit Post Office
Los Angeles 45, California

Approved:

Felix T. Smith, Director
Chemical Physics Division

Copy No. 1

ABSTRACT

Calculations have been made of "flame" (or mixing) dimensions associated with afterburning in rocket exhaust at high altitudes for a hypothetical rocket and trajectory. From these and a given exhaust composition, one can estimate concentrations and times available for reactions of interest. Above some altitudes if observed flame lengths should turn out to be much greater, it would indicate that reaction rates rather than mixing rates were controlling.

Investigation of negative ion formation reactions indicates that they may not be a significant factor in removal of electrons, since dissociative recombination of polyatomic ions is much faster. However, if the production of electrons were mainly due to ionization of alkali metals (which have very low recombination coefficients), the above reactions could be an important electron-removal mechanism.

Calculations have been made of electron densities resulting from thermal ionization of potassium in a rocket engine at various altitudes to provide estimates for comparison and evaluation of the probable significance of other reactions. The estimates indicate that thermal ionization of potassium with typical solid propellants can be a very important source of electrons.

Preliminary investigation of photoionization in rocket exhaust has provided some values of radiation flux density versus altitude for various wavelengths.

Reviewed and approved:

Thomas J. Bellanca

Thomas J. Bellanca, 1st Lt., USAF
Project Administrator

CONTENTS

ILLUSTRATIONS

TABLES

INTRODUCTION

Free electrons in a rocket exhaust stream cause interference in communications with the vehicle and increase its vulnerability to detection. An important source of free electrons is the chemionization produced in the chemical reactions of afterburning as unburned fuel in the exhaust mixes with the ambient atmosphere.

This study, which is a continuation of the work performed under Contract AF 04(647)-751, surveys existing knowledge of afterburning phenomena in rocket exhausts related to the production of ions. The objective is to provide a summary of existing information and to suggest a program of theoretical and experimental research to fill gaps in present knowledge. The over-all aim is to predict or control such ionization.

Efforts will be concentrated on two general areas: (1) fluid dynamics of exhaust jets in the atmosphere at various altitudes, and (2) ionization reactions which may occur during afterburning. The two areas are interrelated and cannot be arbitrarily separated. However, because of the complexity of each field it is desirable to treat them independently insofar as possible.

During this report period, flame length calculations presented in the First Quarterly Report[1] have been treated in more detail, and studies have been made of (a) the possible significance of negative ion formation as electron sinks, (b) the importance of alkali metal contaminants in the propellant, especially in relation to other electron sources, and (c) the possible role of photoionization in rocket exhaust.

Contributions to this report have been made by several people. The following sections are primarily the work of the following individuals:

Negative Ion Formation -- Robert C. Whitten
Thermal Ionization of Alkali Metals -- Carole R. Gatz
Photoionization -- I. G. Poppoff

DISCUSSION

A. Flame Length

The fluid dynamics of an exhaust jet is extremely complicated. However, at high altitudes certain simplifications are admissible. For example, shockwave structures within the jet can be neglected at high altitudes and high velocities.[2,3] Further, at great altitudes[3] (exceeding 60 km) the expansion of the jet to roughly a cylindrical shape is very rapid, so that the boundary of the jet can be approximated by a blunt body with a cylindrical afterbody. Thus, as an approximation the jet is assumed to expand to a cylindrical shape at a distance b from the nozzle exit, and mixing is assumed to begin at x = 0 (see Fig. 1). A shock will be caused by the jet "blunt body," and as the diameter of the expanded jet increases (at higher altitudes due to lower ambient pressure), the shock stand-off distance may actually exceed the length of the rocket, and thus the bow shock from the expanded exhaust jet can occur ahead of the rocket itself. Shock stand-off

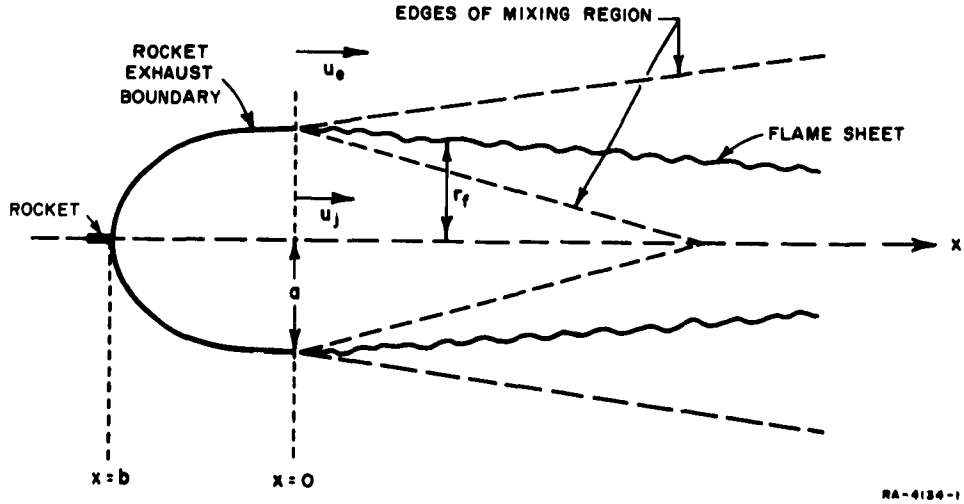

FIG. 1 SCHEMATIC REPRESENTATION OF ROCKET EXHAUST JET

distance Δ for a sphere can be calculated[4] from

$$\Delta/R_0 = 0.143 \exp (3.24/M_\infty^2)$$

where R_0 = radius of the sphere, and M_∞ = free-stream Mach number. For our region of interest, Δ will be roughly 0.15 times the radius of the expanded jet. For our simple model, we will neglect the effects of the rocket body, since the expanded jet will be large in comparison with it.

The pressure at the stagnation point[5] of a hemisphere is assumed to be given by

$$p_{st}/p_\infty = \gamma_\infty M_\infty^2 + 1$$

where p_∞ = free-stream pressure and M_∞ = free-stream Mach number. The pressure decays around the hemisphere toward the cylinder; at the transition, corresponding to x = 0 (Fig. 1), the pressure is assumed[6,7] to be 0.1 p_{st}. Decay to ambient pressure may be assumed to occur at 25-100 diameters behind a sphere,[8] or at about 150 diameters on a cylindrical afterbody.[6,9] In the model for the first calculations of flame length[1] it was assumed that ambient pressure was attained at x = 0 (an unspecified distance b from the front of the expanding exhaust plume) and mixing was assumed to begin at this point. However, if x = 0 is at about 100 expanded jet diameters downstream, one should assume that the disturbance which initiates the growth of turbulent mixing occurs at an earlier point.

For our present model, the distance b to where x = 0 is assumed to be roughly one jet radius, i.e., the blunt portion of the jet is assumed to be roughly hemispherical, the pressure at that point is taken as 0.1 p_{st}, and mixing is assumed to begin there. In order to obtain some dimensions for a jet flow field at high altitudes, calculations by W.T. Lord[10] for a particular rocket and specific trajectory have been used. The semi-divergence angle of the nozzle is 15°, the ratio of the specific heats of the jet gas is 1.2, the velocity of the jet gas at the exit plane is 3000 meters/sec, and the pressure is 1/3 atmosphere. Diameter, 2a, of the expanded jet is presented for different altitudes (Table I, and Fig. 2). The rocket velocity varies linearly with altitude and reaches a value of 7300 meters/sec at 150 km.

Table I

ROCKET EXHAUST AND ATMOSPHERIC CHARACTERISTICS

h	Altitude, km	80	100	110	120	130	140
T_∞	Ambient temperature, ^oK	166	199	287	477	665	850
p_∞	Ambient pressure, mb	1.01×10^{-2}	2.14×10^{-4}	4.91×10^{-5}	2.04×10^{-5}	1.15×10^{-5}	7.50×10^{-6}
ρ_∞	Ambient density gm/cc	2.12×10^{-8}	3.73×10^{-10}	5.93×10^{-11}	1.48×10^{-11}	5.95×10^{-12}	3.02×10^{-12}
v	Rocket velocity m/sec	3890	4870	5350	5840	6320	6820
M_∞	Free-stream Mach No.	14.9	17.1	15.6	13.3	12.0	11.4
u_e	External stream velocity, m/sec	2910	3650	4020	4380	4740	5115
p_j	Jet pressure, mb	2.92×10^{-1}	8.15×10^{-3}	1.56×10^{-3}	4.72×10^{-4}	2.17×10^{-4}	1.28×10^{-4}
T_j	Jet temperature, ^oK	558	374	232	191	168	153
T_e	External stream temp., ^oK	3500	4300	4400	4400	4420	4450
u_j	Jet velocity m/sec	1950	3520	3240	2480	1370	550
u_j/u_e	Velocity ratio	0.68	0.72	0.60	0.42	0.23	0.094
λ	Mean free path, m	3.83×10^{-3}	2.17×10^{-1}	1.36	5.44	13.5	26.4
2a	Jet diameter, m (for 1-meter diameter nozzle)	23	85	160	300	560	1100
L	Flame length, km (for 1-meter-diameter nozzle)	9.1	54	76	87	86	104
L/2a	Flame length/expanded jet diameter	395	635	476	289	154	95

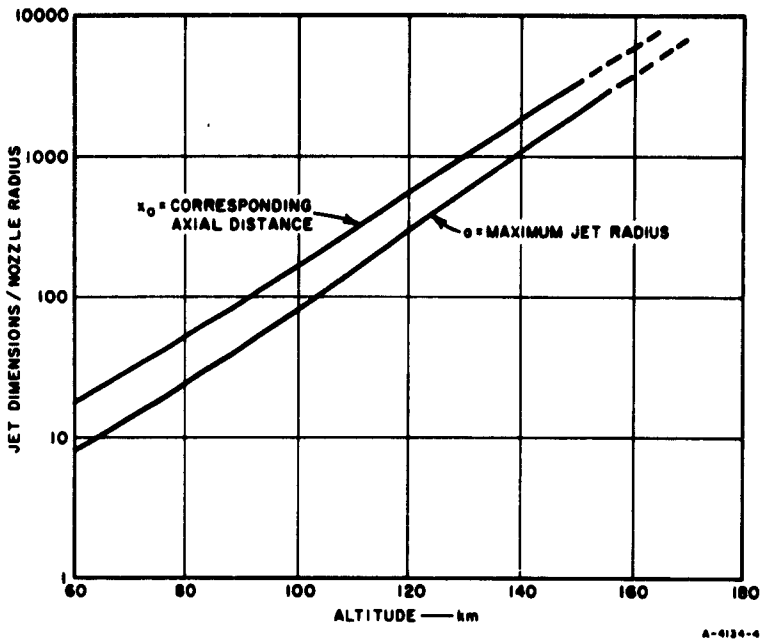

FIG. 2 EXPANDED EXHAUST JET DIMENSIONS (Reference 10)

Expanded jet velocity (average) is obtained from the relation for conservation of mass flux.

$$\rho_j \, u_j \, A_j = M$$

where ρ_j = density, u_j = velocity, and A_j = cross sectional area, each referring to the expanded jet, and M is the mass flowrate at the nozzle. Jet temperature was calculated assuming isentropic expansion. Ambient temperatures, pressures, densities, etc. were taken from the Handbook of Geophysics.[11] External air temperature, T_e, refers to the air within a few jet plume radii, which has been shock-heated in passing through the bow shock, and has been obtained from calculations by Hochstim[12] for equilibrium air. External air velocity, u_e (adjacent to the jet) is assumed to be 0.5 - 0.75 times free-stream velocity, u_∞. For a sphere, Feldman[9] quotes a value of 0.75 u_∞ at the downstream distance where expansion to free-stream pressure has taken place. For purposes of our calculation, we have taken $u_e = 0.75\ u_\infty$.

In order to make some specific calculations of flame lengths and diameters applicable to a rocket rising through the atmosphere, a hypothetical rocket and trajectory have been defined.[10,13] Exhaust composition[13] is given in Table II.

Table II

ROCKET EXHAUST COMPOSITION

Constituent	CO	H_2O	H_2	CO_2	OH	H	O_2	O
Mass % of Total	46	27	1	23	2	0.1	0.6	0.3

Mass ratio air/exhaust required to complete combustion to CO_2 and H_2O -- 1.55

Average molecular weight of exhaust -- 22.1

Exhaust exit temperature -- 1800°K

A calculation of the flame shape in a jet formed by a uniform cylindrical stream of hydrogen surrounded by an ambient paralled high-speed flow of air at a pressure equal to that of the jet (see Fig. 3) has been published.[14] This calculation is based on a theoretical analysis involving a hypothetical model[15] for the eddy viscosity relating it to the eddy viscosity for incompressible flow. The published plot of results of the calculation[14] is presented in Fig. 4. Here r_f is the radius of the flame surface at the axial distance x from the plane where mixing starts (i.e., where x = 0); a is the radius of the jet at x = 0; and u_j/u_e is

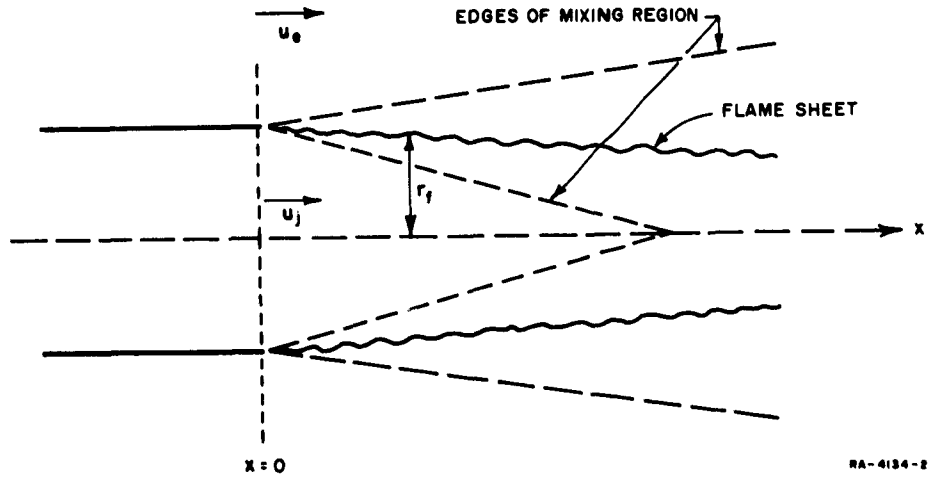

FIG. 3 SCHEMATIC REPRESENTATION OF FLOW (based on Reference 14)

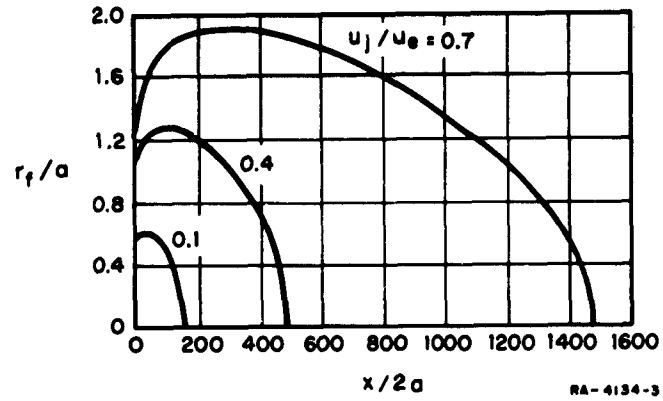

FIG. 4 SHAPE OF FLAME SHEET (Reference 14, Fig. 10)

the ratio of jet velocity to external flow velocity, relative to the nozzle. In Fig. 4 it is assumed that the chemical reaction rate is infinite and that the turbulent flow and mixing process control the flame surface location.

Flame lengths and maximum diameters can be obtained from Fig. 5 (derived from Fig. 4) as a function of u_j/u_e. Flame length L (or L/2a in dimensionless form) is defined as the value of x (or x/2a) when r_f/a is zero. However, these values refer to the following special conditions: a jet of hydrogen gas at 1300°K, external flow of air at 1600°K, both at 1-atmosphere pressure, and ambient air temperature (far from the exhaust flow field) of 282°K. Application of Libby's method to other gases and conditions (different molecular weights, concentrations, temperatures, etc.) requires very lengthy calculations, unless one can use some simple theory of mixing and assume some relation between it and Libby's theory. This has been done to provide a preliminary test of

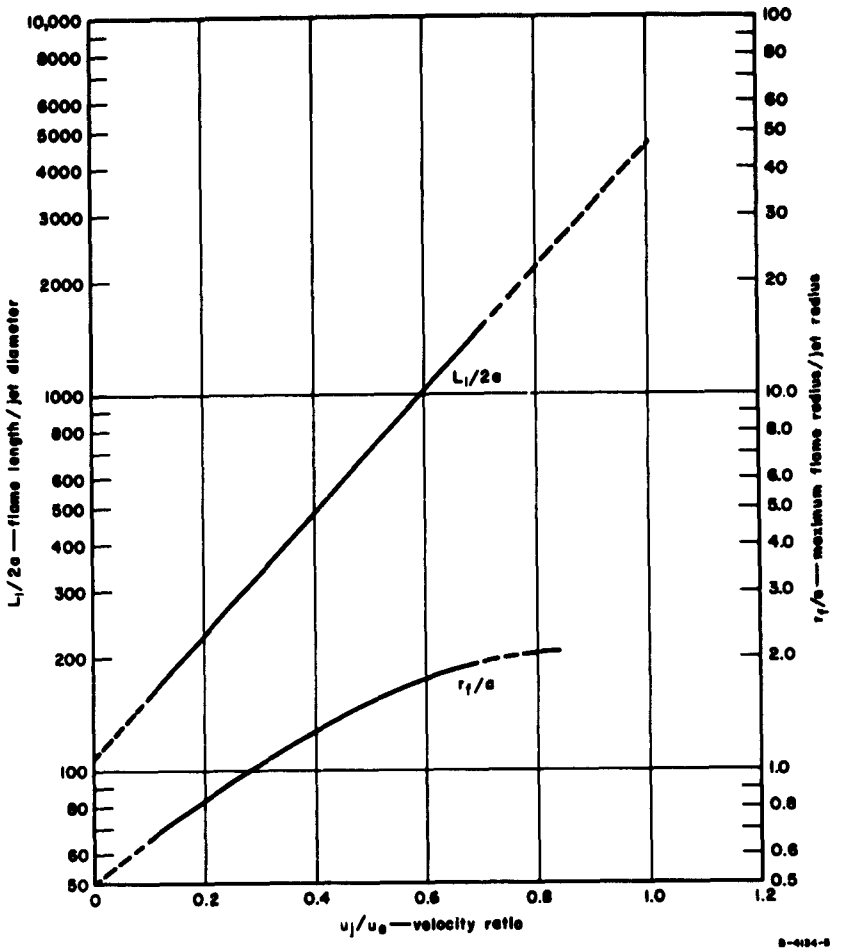

FIG. 5 FLAME DIMENSIONS (derived from Fig. 4)

Libby's method. Use has been made of some work by Ricou and Spalding[16] on determination of entrainment length, y, for jets. The assumption is made that for two different sets of conditions for jets (identified by subscripts 1 and 2),

$$L_2/L_1 = y_2/y_1 \qquad \text{or} \qquad L_2 = \frac{y_2}{y_1} L_1 \qquad (1)$$

where, L_2 is the flame length sought, L_1 is the value obtained from Fig. 5, and y_2 and y_1 are the corresponding entrainment lengths.

The calculation of the entrainment length y is based upon the following equation:[16]

$$\frac{m_e}{m_j} + 1 = 0.32 \frac{y}{2a} \left(\frac{\rho_e}{\rho_j}\right)^{\frac{1}{2}} \qquad (2)$$

where m_e is the mass flux of ambient air which has been entrained by the jet at downstream distance y, m_j is the mass flux of the original jet (i.e., before any mixing has occurred) , and ρ_e and ρ_j are the densities of the unmixed ambient and jet streams respectively. In this report the definitions of y and m_e/m_j are further restricted to the special values where $M = m_e/m_j$ represents a stoichiometric ratio for whatever gases are considered. Also let $P = \rho_e/\rho_j$. Then one can solve equation (2) for the appropriate values of y, and obtain

$$\frac{y_2}{y_1} = \frac{M_2 + 1}{M_1 + 1}\left(\frac{P_2}{P_1}\right)^{-\frac{1}{2}}$$

Substituting values corresponding to conditions for Figs. 4 and 5, one obtains

$$\frac{y_2}{y_1} = 0.0513\ (M_2 + 1)P_2^{-\frac{1}{2}} \qquad (3)$$

An indication of the maximum altitude at which continuum theory can be expected to hold can be seen from comparison of ambient mean free path, λ, with expanded jet diameter, 2a, Table I. If one employs the criterion that the characteristic dimension should be at least 100 times the mean free path, the following conclusions can be drawn: for the jet as a simple blunt body, continuum theory may hold to an altitude of 110-120 km; for turbulent mixing assuming a typical eddy size of one-tenth the jet diameter as the characteristic dimension, continuum theory may hold only to around 90 km; for a shock standoff distance of 0.075 times the jet diameter as characteristic dimension, the corresponding altitude is somewhere near 90 km. Of course, the mean free path in the shock layer itself is much smaller than ambient (by a factor of 20-30) because of the high density. As the size of the expanded jet depends upon the size

and nature of the rocket and its trajectory, these factors must be considered in any estimate of the altitude. A quite different criterion for the maximum altitude to which continuum theory should apply is the relaxation time,[17] i.e., the mean time between collisions. For large relaxation times, small disturbances will propagate in both longitudinal and transverse modes. When air density becomes less than about 10^{-10} atmosphere (or 10^{-7} mb), undamped small disturbance propagation tends to occur. For the ambient air, this corresponds to about 105 km. In the jet, because the density is higher due to higher pressure and lower temperature, the corresponding altitude is higher.

At the present time we lack field data in "flame" lengths for various altitudes in the range considered here, and so have no way of comparing with observed trends of flame lengths versus altitude. Estimates can be made of available times for reaction. Dividing the calculated lengths by the corresponding rocket velocities provides maximum times of mixing; but the reaction time must be much smaller (say not more than one-tenth as great) in order not to increase the flame length, which is calculated on the assumption of a reaction time small compared to the mixing time. Rough values of reaction times (dividing the mixing time by 10) are then found to vary from 0.23 sec at 80 km to 1.5 sec at 140 km. These times can be used at least tentatively in evaluating the significance of various electron production and removal reactions at different altitudes.

B. Negative Ion Formation

A previous study[2] of ionization, including negative ions in the afterburning regions of rocket exhaust, described qualitatively some of the effects which one would expect to find there. However, it did not consider many of the finer details of the ionic processes such as the possible importance of negative ion formation as a mode of electron removal. Some of these details will be developed in the following, and from the results we shall make order of magnitude estimates of negative ion concentrations, required electron production rates for a given level of ionization, etc.

In order to compute the concentrations of negative ions present in the plume one must know or at least have a reasonable model of the rocket exhaust composition. Of the various estimates which have been made we shall employ that proposed by Boynton and Neu[13] for a liquid fueled rocket (Table II). In addition we shall assume that the plume constituents mix thoroughly with the ambient atmosphere and that the pressure and temperature in the afterburning region are equal to the ambient pressure and temperature, given by the ARDC 1959 Model Atmosphere.[18] Because of only partial mixing of the rocket exhaust with the atmosphere and the presence of shockwaves which result in higher pressures and temperatures in regions of the plume, these assumptions are not completely justified. However, in view of the very crude estimates of rate constants which we shall introduce later, it is considered unlikely that errors associated with these assumptions will be greater than those associated with the rate constants. The lifetime of the afterburning region is estimated to be of the order of 1 sec.

Electron removal processes are basically of two types, recombination and attachment. Before discussing the former we shall consider the formation and destruction of negative ions. The most important such processes are

Radiative Attachment

$$O_2 + e \rightarrow O_2^- + h\nu \qquad (a1)$$

$$O + e \rightarrow O^- + h\nu \qquad (a2)$$

$$H + e \rightarrow H^- + h\nu \qquad (a3)$$

Collisional Attachment

$$O_2 + O_2 + e \rightarrow O_2^- + O_2 \qquad (b1)$$

$$O + O_2 + e \rightarrow O^- + O_2 \qquad (b2)$$

Photodetachment

$O_2^- + h\nu \rightarrow O_2 + e$ (c1)

$O^- + h\nu \rightarrow O + e$ (c2)

$H^- + h\nu \rightarrow H + e$ (c3)

$OH^- + h\nu \rightarrow OH + e$ (c4)

$NO_2^- + h\nu \rightarrow NO_2 + e$ (c5)

$O_3^- + h\nu \rightarrow O_3 + e$ (c6)

Collisional Detachment

$O_2^- + O_2 \rightarrow O_2 + O_2 + e$ (d1)

$O_2^- + O \rightarrow O_3 + e$ (d2)

$O^- + O \rightarrow O_2 + e$ (d3)

$H^- + H \rightarrow H_2 + e$ (d4)

$OH^- + H \rightarrow H_2O + e$ (d5)

$N + NO_2^- \rightarrow N_2 + O_2 + e$ (d6)

$O + H^- \rightarrow OH + e$ (d7)

$O + O_3^- \rightarrow O_2 + O_2 + e$ (d8)

$H + O_3^- \rightarrow OH + O_2 + e$ (d9)

Charge Transfer and Ion-Atom Interchange

$O_2^- + O \rightarrow O_2 + O^-$ (e1)

$O_2^- + O + O_2 \rightarrow O_2 + O_3^-$ (e2)

$O_2^- + N + M \rightarrow NO_2^- + M$ (e3)

$O^- + OH \rightarrow O + OH^-$ (e4)

$H^- + OH \rightarrow H + OH^-$ (e5)

$O_2^- + OH \rightarrow O_2 + OH^-$ (e6)

$O_2^- + H \rightarrow O_2 + H^-$ (e7)

$O^- + O_2 + O_2 \rightarrow O_2 + O_3^-$ (e8)

$H^- + O \rightarrow O^- + H$ (e9)

Reaction (e4) is energetically permitted only if the electron affinity of O^- is less than 1.8 ev. Although the photodetachment experiments of Branscomb and co-workers[19] indicated that this condition is satisfied, more recent work by Schulz[20] (1962) yields an electron affinity of .2 ev. Because we are not yet certain which value applies to the O^- in the ionosphere, we do not know whether the process is possible or not; for present purposes we shall assume that it is. Some of the rate constants associated with the reactions listed above have been measured. Estimates of others are based on typical experimental values associated with similar reactions. Temperature dependence has been neglected because of the probable absence of activation energies; the error so introduced is expected to be less than other uncertainties in the rate constants. The experimental results and estimates are shown in Table III.

Table III

RATE CONSTANTS

Process	Rate Constant	Value	Reference
a1	β_1	10^{-15} cm^3/sec	Branscomb et al.[21] (1958), using photodetachment data and principle of detailed balancing
a2	β_2	10^{-19} cm^3/sec	Estimated by Poppoff and Whitten,[22] (1962) using photodetachment data and principle of detailed balancing (Burch et al.,[19] 1958)
a3	β_3	10^{-16} cm^3/sec	Same as a2, using data of Smith and Burch[23] (1959)
b1	k_1	10^{-30} cm^6/sec	Chanin et al.[24] (1959)
b2	k_2	10^{-31} cm^6/sec	Estimate, based on idea that b1 probably involves resonance and thus should be perhaps an order of magnitude faster
c1	ρ_1	0.1 sec^{-1}	Estimate (Poppoff and Whitten,[22] (1962))
c2	ρ_2	1.4 sec^{-1}	Branscomb et al.[21] (1958)
c3	ρ_3	8 sec^{-1}	Computed from results of Smith and Burch[23] (1959)
c4	ρ_4	10^{-2} sec^{-1}	Estimate
c5	ρ_5	10^{-3} sec^{-1}	Estimate
c6	ρ_6	10^{-2} sec^{-1}	Estimate

Table III (Concluded)

Process	Rate Constant	Value	Reference
d1	γ_1	10^{-20} cm^3/sec	Phelps and Pack[25] (1961)
d2	γ_2	10^{-13} cm^3/sec	Estimate; could well be an order of magnitude larger
d3	γ_3	10^{-13} cm^3/sec	Same as d2
d4	γ_4	10^{-13} cm^3/sec	Same as d2
d5	γ_5	10^{-13}	Same as d2
d6	γ_6	10^{-13}	Same as d2
d7	γ_7	10^{-13}	Same as d2
d8	γ_8	10^{-13}	Same as d2
d9	γ_9	10^{-13}	Same as d2
e1	k_1	10^{-11}	Estimate; rate constants for positive ion charge transfer processes in atmosphere have been found to be of order 10^{-11} cm^3/sec, Dickinson and Sayers,[26] (1960)
e2	k_2	10^{-32} cm^6/sec	Estimate; maybe as large as 10^{-31} cm^6/sec
e3	k_3	10^{-31} cm^6/sec	Estimate
e4	k_4	10^{-11} cm^3/sec	Same as e1
e5	k_5	10^{-11} cm^3/sec	Same as e1
e6	k_6	10^{-11} cm^3/sec	Same as e1
e7	k_7	10^{-11} cm^3/sec	Same as e1
e8	k_8	10^{-32} cm^3/sec	Same as e2
e9	k_9	10^{-11} cm^3/sec	Same as e1

For a given electron density [e] this set of constants can be used in conjunction with the corresponding rate equations and the concentrations of neutral species given in Table IV to compute the concentrations of the various species of negative ions. Actually we also need to know the ion-ion recombination coefficients α_i and the positive ion concentrations $[X^+]$. For our purposes, however, neglect of this term will not materially affect the final results. After carrying out the computations for the negative ion concentrations after 1 sec, we obtain the results presented in Table V.

Table IV

CONCENTRATIONS OF NEUTRAL SPECIES (cm^{-3})
Minzner,[18] (1959); Handbook of Geophysics,[11] (1960);
Boynton and Neu,[13] (1960)

Altitude	$[O_2]$	$[N_2]$	$[O]$	$[N]$	$[OH]$	$[H]$
80 km	10^{14}	4×10^{14}	10^{12}	10^{7}	10^{12}	10^{11}
100 km	10^{12}	6×10^{12}	3×10^{12}	10^{7}	10^{11}	5×10^{9}
130 km	10^{10}	10^{11}	10^{11}	10^{7}	10^{9}	5×10^{7}

Table V

NEGATIVE ION CONCENTRATIONS[a]

Altitude	$[O_2^-]$	$[O^-]$	$[H^-]$	$[OH^-]$	$[NO_2^-]$	$[O_3^-]$
day[b]						
80 km	200	350	50	10^{5}	100	$\ll 1$
100 km	0.3	10^{4}	0.1	10^{4}	$\ll 1$	$\ll 1$
130 km	$\ll 1$	10^{3}	$\ll 1$	10	$\ll 1$	$\ll 1$
Night[b]						
80 km	200	4×10^{3}	10^{4}	2×10^{5}	100	$\ll 1$
100 km	0.3	2×10^{4}	0.1	2×10^{4}	$\ll 1$	$\ll 1$
130 km	$\ll 1$	10^{3}	$\ll 1$	10	$\ll 1$	$\ll 1$

[a]We are assuming that $[e] = 10^{7}$ cm^{-3}, Smith,[2] (1961)

[b]Photodetachment ceases at sunset and thus causes the negative ion concentrations to rise

From the results of Table V we can conclude that $[OH^-]$ and $[O^-]$ are expected to be the most important negative ions in the rocket plume. Although an increase in the charge transfer rate constants will have the effect of increasing the relative concentrations of NO_2^- the net effect will be small since it is extremely unlikely that the true values of the k's will be more than about one order of magnitude larger than those listed in Table III. Increasing the values of the collisional detachment coefficients γ will have an important effect, particularly at night, by reducing the total negative ion concentrations, perhaps by an order of magnitude below those given in Table V.

Recombination can occur by either of two mechanisms, dissociative, e.g.,

$$O_2^+ + e \rightarrow O + O \qquad (5a)$$

or ion-ion, e.g.,

$$O_2^+ + O_2^- \rightarrow O_2 + O_2 \ , \qquad (5b)$$

which are related to an effective recombination coefficient α_{eff} by the equation

$$\alpha_{eff} = \alpha_D + \lambda \alpha_i \qquad (6)$$

where λ is the negative ion to electron concentration ratio. For some of the ions of interest in the plume (e.g., CHO^+, H_3O^+) α_D is probably of the order 10^{-6} cm^3/sec while α_i is expected to be considerably smaller, i.e., $\sim 10^{-8}$ cm^3/sec.[27] Using the estimates of negative ion concentrations in Table V, we see that the dissociative mode is much the faster recombination mechanism for the polyatomic ions and we can neglect negative ion formation as a deionization process in the afterburning region except in the case of alkali metal ions which cannot undergo dissociative recombination. Because of the unavailability of the dissociative mode the effective recombination coefficient for these species is expected to be much smaller, probably of the order of 10^{-10} cm^3 sec^{-1}.

The dominant ionization mechanism in the plume is thought to be chemionization, specifically[2]

$$CH + O \rightarrow CHO^+ + e \qquad (7)$$

The dissociative recombination coefficient of a complex ion of this type is probably of the order 10^{-6} cm^3/sec, thus requiring an electron production rate of $\sim 10^8$ cm^{-3} sec^{-1} to produce electron concentrations of the order 10^7 cm^{-3}. Assuming that the rate constant of process (7) is of the order 10^{-12} cm^3 sec^{-1}, which is reasonable for two-body chemical reactions, one finds that concentrations of CH of $\sim 10^8$ cm^{-3} are required. This is equivalent to ~ 0.3 ppm at 80 km, ~ 3 ppm at 100 km, and ~ 5000 ppm at 130 km. The estimates at 80 and 100 km appear reasonable but that at 130 km is undoubtedly much too large. We conclude that at an altitude in the region of about 150 km the electron density in the rocket plume probably approximates the ambient concentration.

If all of the positive ions were alkali metal ions, e.g., Na^+, K^+, a much smaller ionization rate would be required to maintain a given electron concentration; this is due to the smaller effective recombination coefficients previously discussed. Whether or not the ionization due to alkali metals in liquid fuel rockets is large enough to rival the chemionization process, equation (7), is not known. If it is, negative ions must be of great importance to the ionization properties of the plume. This point deserves further investigation. Alkali metals are present as impurities in fuels, and some atoms will be thermally ionized in the rocket engine. There is also the possibility of photoionization at high altitudes. Also formation of Cl^- may be important for aluminum perchlorate propellants, especially at lower altitudes where Cl concentration is much greater than O concentration.

C. Thermal Ionization of Alkali Metals

A high concentration of electrons may be present in the exhaust gases emerging from a rocket motor. A principal source of these electrons is thermal ionization of species of low ionization potential, such as

alkali metal contaminants in the propellant. High levels of ionization presumably are attained at the high temperature of the combustion chamber; some of this ionization may be frozen during nozzle expansion and during subsequent expansion of the plume to ambient pressure.

Electrons may also be produced by interactions of the plume with the external environment. If processes such as impact ionization, photoionization, and chemionization are to be significant sources of ionization, they must produce electrons in greater concentrations than the background electron density due to thermal ionization.

We shall formulate approximate expressions for the fractional ionization of potassium in the exhaust and for the resultant electron density in the expanded plume, due to thermal ionization in the rocket. We can then estimate electron densities in the exhaust from this source under various conditions. Such estimates also provide a criterion for evaluating the significance of other sources of ionization in the exhaust plume.

The equilibrium constant K_{eq} for

$$A \rightleftarrows A^+ + e \qquad (1)$$

can be calculated by the Saha equation, which for alkali metals is

$$K_{eq} = \frac{[A^+]n_e}{[A]} = 2.41 \times 10^{15}\ T^{3/2}\ e^{-I/kT} \qquad (2)$$

where T is the temperature (^{o}K), I is the ionization potential of A, k is Boltzmann's constant, n_e is the electron density (cm^{-3}), and the brackets denote concentrations per cm^3.

In the absence of any other process producing or removing electrons, $[A^+] = n_e$, and the electron density is given by

$$n_e = \{[A]\ 2.41 \times 10^{15}\ T^{3/2}\ e^{-I/kT}\}^{\frac{1}{2}} \qquad (3)$$

and the fractional ionization of A by

$$\frac{[A^+]}{[A]} = \left(\frac{2.41 \times 10^{15}\ T^{3/2}\ e^{-I/kT}}{[A]}\right)^{\frac{1}{2}} \qquad (4)$$

The concentration of A is

$$[A] = f_A \frac{P}{kT} \qquad (5)$$

where f_A is the number fraction of A in the gas and P is the total pressure.

We assume that the ionization of potassium at the exit plane of the motor can be described as equilibrium ionization at some temperature T_i. This effective ionization temperature may not be the actual temperature at the exit plane, since ionization may have been frozen at some earlier stage of nozzle expansion. Our ability to predict T_i is therefore limited, but T_i will lie between throat and exit plane temperatures.

The equilibrium constant for potassium, calculated from equation (2) for several values of T_i, is given in Table VI. We combine equations (4) and (5) to obtain an expression for the fractional ionization of potassium,

$$\frac{[K^+]}{[K]} = \left(\frac{K_{eq}}{[K]}\right)^{\frac{1}{2}} = \left(\frac{K_{eq}\ k\ T_i}{f_K\ P_i}\right)^{\frac{1}{2}} . \qquad (6)$$

Table VI

EQUILIBRIUM CONSTANT FOR $K \rightleftarrows K^+ + e$ FOR VARIOUS TEMPERATURES

T_i	K_{eq}
1500	4.0×10^{5}
2000	2.7×10^{9}
2500	5.7×10^{11}
3000	2.1×10^{13}

The fractional ionization thus depends on the potassium concentration and the effective ionization pressure as well as on T_i. In Table VII are given values of $[K^+]/[K]$ calculated for typical conditions, $f_K = 100$ parts per million by number, and $P_i = 5$ psia. For conversion to other conditions, note that $[K^+]/[K]$ scales as $(f_K P_i)^{-\frac{1}{2}}$.

Table VII

FRACTIONAL IONIZATION OF POTASSIUM AT VARIOUS IONIZATION TEMPERATURES

T_i	1500	2000	2500	3000
$[K^+]/[K]$	5×10^{-5}	5×10^{-3}	7×10^{-2}	5×10^{-1}

The calculated values in Table VII, as would be expected, show a general tendency toward increasing fractional ionization as T_i increases. These values should not be compared in detail because of the arbitrary assumption that $P_i = 5$ psia. However, an alternative assumption of constant number density rather than constant pressure would change the relative values at the highest and lowest temperatures in Table VII by

a factor of only $\sqrt{2}$. We can conclude that any other process of potassium ionization which produces a fractional ionization of less than 10^{-5} is probably not significant in comparison with thermal ionization.

If we assume the fractional ionization at the exit plane, as estimated in Table VII, is frozen during plume expansion to ambient pressure, then we can estimate typical electron densities in the plume using equation (3). The value of [K] for the expanded plume is given by

$$[K] = \frac{f_K}{T_e} P_e \times 8 \times 10^{21} \quad . \qquad (8)$$

Approximate values for P_e, the ambient pressure in atmospheres, are given for various altitudes in Table VIII. These data are slightly different from those used in the first section, but the differences are not significant for our purposes. The temperature of the expanded plume, T_e, can be calculated for a particular motor at a particular altitude for a specific expansion model (such as assumed isentropic expansion). We shall assume $T_e = 100^{o}K$ in order to calculate typical values of n_e. Note that n_e scales as $(T_e)^{-\frac{1}{2}}$. The calculated electron densities in the expanded exhaust at various ionization temperatures and altitudes are given in Table IX; as before, we have assumed f_K = 100 ppm by number and P_i = 5 psia.

Table VIII

AMBIENT PRESSURE AT VARIOUS ALTITUDES

Altitude (km)	Pressure (atm)
200	10^{-9}
150	3×10^{-9}
100	10^{-7}
80	10^{-5}
60	2×10^{-4}
40	3×10^{-3}

Table IX

CALCULATED ELECTRON DENSITIES (cm^{-3}) IN THE EXHAUST AT VARIOUS IONIZING TEMPERATURES AND ALTITUDES

Altitude (km)	T_i			
	1500	2000	2500	3000
200	2.8×10^{2}	3.6×10^{4}	5.6×10^{5}	3.8×10^{6}
150	1.1×10^{3}	1.1×10^{5}	1.7×10^{6}	1.2×10^{7}
100	3.8×10^{4}	3.6×10^{6}	5.6×10^{7}	3.2×10^{8}
80	3.8×10^{6}	3.6×10^{8}	5.6×10^{9}	3.8×10^{10}
60	7.5×10^{7}	7.2×10^{9}	1.1×10^{11}	7.7×10^{11}
40	1.1×10^{9}	1.1×10^{11}	1.7×10^{12}	1.2×10^{13}

At a given altitude, n_e increases with ionization temperature, although the calculated values are dependent on the assumed P_i, as before. Since we have assumed a constant total number of electrons in the plume for a particular T_i, the electron density naturally decreases with ambient pressure as the altitude increases. However, since T_e also decreases with pressure, the rate of decrease of n_e with increasing altitude is not as large as indicated by the values in Table IX.

Many assumptions and approximations, in addition to those already mentioned, are implicit in the above calculations. Some of these will now be specified in more detail. Sources of electrons other than potassium have been neglected. With its relatively low ionization potential, potassium in the amounts typically present in solid propellants would quite reasonably be expected to dominate thermal ionization. Electron sinks other than K^+ have been ignored in the formulation of equilibrium ionization. The most serious effect of this type is probably due to the presence of electron-attaching species such as Cl. The effect of equilibria such as $Cl^- \rightleftarrows Cl + e$ can be calculated in theory. The result would be lower values for n_e and higher values for $[K^+]/[K]$ than

given in tables VI-IX. Since equilibrium shifts toward detachment with increasing temperature, the assumption of neglecting attachment is better at higher temperatures.

It has been assumed that the potassium is available as atoms in the vapor phase. One should really consider dissociation equilibria for the potassium compounds in the fuel and other chemical sinks for potassium, such as $KOH \rightleftarrows K + OH$. Neglecting such effects, as in the above calculations, can be regarded as merely a limitation on our ability to estimate [K] accurately. However, this should be given careful consideration in future studies.

The assumption that ionization is frozen during plume expansion seems reasonable for conditions of interest. If K^+ and electrons undergo 3-body recombination with a rate constant of about 10^{-27} cm^6 sec^{-1}, then the time required to reduce the electron density by one-half is given by

$$t_{\frac{1}{2}} = (10^{-27}[M]n_e)^{-1} \qquad (9)$$

If $n_e = 10^{10}$ cm^{-3} and $[M] = 10^{17}$ cm^{-3} (0.01 atm at 300°K), then $t_{\frac{1}{2}} \sim 1$ second, a time which is long enough compared with expansion time for recombination to be neglected.

We concluded that the amount of potassium ordinarily contained in solid propellants may produce electron densities in the exhaust plume at low altitudes which are sufficiently high to cause an attenuation problem. Nevertheless because of the uncertainties mentioned above one cannot make a positive prediction. As the exhaust temperature increases, this effect persists to higher altitudes. The lower temperature in the combustion chamber and the lower concentration of alkali metals in liquid fuel rockets lead to considerably lower calculated values for thermal ionization.

The purpose of these approximate calculations is not only to indicate conditions under which thermal ionization leads to large electron densities, but also to provide a criterion for estimating the

importance of other ionization mechanisms. Obviously, only those reactions which can produce electrons in larger concentrations than the background thermal ionization can have an important effect on the ionization level of the exhaust.

For example, consider a general process:

$$X^* + K \rightarrow X + K^+ + e \qquad (10)$$

where X* is an excited species whose excitation energy is greater than the ionization potential of potassium. If this process is to have a significant effect on the electron density, the concentration of X* must obviously be larger than the background electron density, or its rate of production in the exhaust must be much larger than the required electron production rate. The electron production rate by this process must exceed the recombination rate if an increase in electron density is to occur. As an upper limit to the recombination rate assume dissociative recombination with a recombination coefficient of 10^{-6} cm^3 sec^{-1} can occur. Then, if the rate constant for reaction (10) is about 10^{-12} cm^3 sec^{-1}, we require that

$$10^{-12}[X^*][K] > 10^{-6}[K^+]^2 \ . \qquad (11)$$

If $[K^+]/[K] \sim 10^{-4}$ and $[K] \sim 10^{10}$ cm^{-3}, then equation (11) indicates that a concentration $[X^*] > 10^8$ cm^{-3} is sufficient to increase the electron density.

A more convenient method for applying this criterion may be to define a characteristic time for electron loss (by recombination or diffusion) in the plume. Then, if the electron production rate by a particular mechanism can be estimated, the total ionization per unit volume during this characteristic time can be compared directly with the background thermal ionization. For example, the rate of photoionization of potassium by solar radiation is $\frac{FQ[K]}{I}$ sec^{-1}, where F is the total flux per cm^2 per sec in the appropriate wavelength region, Q is an averaged photoionization cross section, and I is the ionization potential. If the background fractional ionization of potassium is

$[K^+]/[K]$, the time required for photoionization to increase the ionization significantly is $\frac{[K^+]I}{[K]FQ}$. This must be less than the characteristic time, if photoionization is to be an important process.

D. Photoionization

The importance of photoionization effects in missile exhaust plumes is being explored. A preliminary look at this problem indicates that sufficient solar energy in the ultraviolet wavelengths may penetrate to altitudes at which rocket motors are still burning or outgassing. The study is, of course, restricted to those photon energies that are capable of photoionization.

Table X summarizes estimates, based on rocket data,[28,29,30] of altitudes at which 1/e of the solar flux (of given wavelength) incident to the top of the atmosphere will penetrate. The maximum ionization potentials that can be supplied at the 1/e penetration altitude by the photons are also listed, along with estimated fluxes and an indication of some common substances that could be ionized at or above the indicated altitudes. Except for Lyman-α of hydrogen, the values are averages and do not represent specific strong line emission.

Calculation of ionization rates is rather lengthy and requires compilation of considerable data because the spectral distribution of radiation intensity varies with altitude, and both the spectral radiation intensity and the photoionization cross sections vary (often in a rather complicated manner) with wavelength. However it may be of interest to consider some examples of rate of ionization per unit wavelength interval for NO, K, and CO, using corresponding absorption cross sections of 2×10^{-18} cm^2, 6×10^{-21} cm^2, and 1.6×10^{-17} cm^2, respectively.[31,32] These cross sections correspond to the wavelengths attenuated to 1/e of the initial flux.

Table X

ESTIMATES OF PHOTOIONIZATION PARAMETERS

Solar Radiation Attenuated to 1/e at Altitude (km)	Wavelength of Attenuated Radiation (A)	Photon Energy of Radiation (ev)	Examples of Substances Ionized at or above 1/e Penetration Altitude	Approximate Average* Spectral Radiation Intensity 1/e Penetration Altitude (ergs/cm^2 sec A)
23	3000	4.1	Cs	16.5
30	2800	4.4	K	8.5
40	2600	4.8		5.2
40	2400	5.2	Na	2.5
33	2200	5.6	Li	2.3
42	2000	6.2	Al, Ca	0.51
82	1800	6.9		0.14
110	1600	7.8	Ni, Mg	0.023
112	1400	8.9	Fe, Co	1.9×10^{-3}
≈75	Lα		NO	1.87
70-110	1200	10.3		4.2×10^{-2}
95	1000	12.4	C_2, O_2, NO_2, NH_3, Parafines	1.3×10^{-3}
130	800	15.5	H, O, Cl, N, H_2, N_2, Cl_2, CO, OH, H_2O, CO_2, CH_4	9×10^{-4}
162	600	20.6	F	7.3×10^{-4}
150	400	31		10^{-3}
110	44-60	300-205		10^{-2}
100-115	8-20	1500-620		2×10^{-3}
65-100	2-8	6200-1500		10^{-3}

*Not uniformly averaged some 50A, 16A, 12A increments.

Examples of ionization rates that may be possible to obtain at the 1/e penetration altitudes are as follows.

1. NO: Can be ionized by radiation shorter than approximately 1200A (Lyman α would be the major radiation for this reaction). Two ion pairs cm^{-3} sec^{-1} A^{-1} would be produced per 10^7 cm^{-3} NO molecules.

2. K: Four ion pairs cm^{-3} sec^{-1} A^{-1} would be produced per 10^9 cm^{-3} K atoms.

3. CO: Five ion pairs cm^{-3} sec^{-1} A^{-1} would be produced per 10^{10} cm^{-3} CO molecules.

During the next quarter, attempts will be made to determine the order of magnitude of concentrations of ionizable constituents that can be expected to exist in missile plumes at various altitudes. If consideration of these data still indicates that photoionization may be important, a more thorough study of the problem will be planned. In the meanwhile, compilation of radiation flux and photoionization cross section data will continue.

BIBLIOGRAPHY

1. Schadt, Conrad F., Ionization in Afterburning Rocket Exhausts, Quarterly Report No. 1, Part 1. Technical Note SSD-TDR-62-163, Stanford Research Institute, October 1962.

2. Smith, F. T., Ionization in Afterburning Rocket Exhausts, Quarterly Report No. 2, Technical Note BSD-TR-61-26, Stanford Research Institute, August 1961.

3. Gold, H., Flow Regimes of a Rocket Exhausting into a Hypervelocity Stream at High Altitude, Contract SD66, OHD Data Collection and Analysis Center, Stanford Research Institute, August 1962.

4. Ambrosio, Alphonso and Andrzej Wortman, Stagnation point shock detachment distance for flow around spheres and cylinders, ARS Journal 32, 281 (1962).

5. Wang, C. J. and J. B. Peterson, Spreading of supersonic jets from axially symmetric nozzles, Jet Propulsion 28, 321, (1958).

6. Casaccio, Anthony, Theoretical pressure distribution on a hemisphere-cylinder combination, Aerospace Sci. 26, 63 (1959).

7. Kemp, Nelson H., Peter Rose, Ralph W. Detra, Laminar heat transfer around blunt bodies in dissociated air, J. Aerospace Sci. 26, 421, (1959).

8. Lees, Lester and Leslie Hromas, Turbulent diffusion in the wake of a blunt-nosed body at hypersonic speeds, J. Aerospace Sci. 29, 976, (1962).

9. Feldman, Saul, Trails of Axi-Symmetric Hypersonic Blunt Bodies Flying through the Atmosphere, Research Report 82, Avco-Everett Research Laboratory, December 1959.

10. Lord, W. T., On axisymmetrical Gas Jets, with Application to Rocket Flow Fields at High Altitudes, Report No: AERO. 2626 Royal Aircraft Establishment (Farnborough) July 1959.

11. Handbook of Geophysics (Revised Edition), U.S. Air Force, MacMillan, New York, 1960.

12. Hochstim, A. R., Gas Properties Behind Shocks at Hypersonic Velocities, Report No. ZPh (GP)-002, Convair, San Diego, January 30, 1957.

13. Boynton, Frederick, P. and John T. Neu , Rocket Plume Radiance V. Calculation of Adiabatic Flame Temperatures of Afterburning Rocket Exhaust, Report No. ERR-AN-011, Convair-Astronautics, 16 May 1960.

14. Libby, Paul A., Theoretical analysis of turbulent mixing of reactive gases with application to supersonic combustion of hydrogen, ARS Journal 32, 388, (1962).

15. Ling, T., and P. A. Libby, Remarks on the eddy viscosity in compressible mixing flows, J. Aerospace Sci. 27, 797 (1960).

16. Ricou, F. R. and D. B. Spalding, Measurements of entrainment by axisymmetrical turbulent jets, J. Fluid Mechanics, 11, 21 (1961).

17. Logan, J. G., Relaxation time in rarefied gas flows, ARS Journal 32, 1099, (1962).

18. Minzner, R. A., K. S. W. Champion, and H. L. Pond, The ARDC Model Atmosphere, 1959; Geophysics Research Directorate Report No. 115, Air Force Cambridge Research Center, Bedford, Mass (August, 1959).

19. Burch, D. S., S. J. Smith, and L. M. Branscomb, Photodetachment from O_2^-, Phys. Rev. 112, 171 (1958).

20. Schulz, G. J., Cross section and electron affinity for O^- ions from O_2, CO, CO_2 by electron impact, Phys. Rev. 128, 178 (1962).

21. Branscomb, L. M., D. S. Burch, S. J. Smith, and S. Geltman, Photodetachment cross section and electron affinity of atomic oxygen, Phys. Rev. 111, 504 (1958).

22. Poppoff, I. G., and R. C. Whitten, Determination of Ionosphere Recombination Coefficients, Stanford Research Institute, September 1962.

23. Smith, S. J. and D. S. Burch, Relative measurements of the photodetachment cross section for H^-, Phys. Rev. 116, 1125 (1959).

24. Chanin, L. M., A. V. Phelps, and M. A. Biondi, Measurement of the attachment of slow electrons in oxygen, Phys. Rev. Letters 2, 344 (1959).

25. Phelps, A. V. and J. L. Pack, Collisional detachment in molecular oxygen, Phys. Rev. Letters 6, 111 (1961).

26. Dickinson, P. H. G. and J. Sayers, Ion charge exchange reactions in oxygen afterglows, Proc. Phys. Soc. 76, 137 (1960).

27. Naurocki, P. J., Reaction Rates, Scientific Report, Geophysics Corporation of America, January 1961.

28. Hall, L. A., K. R. Damon, and H. E. Hinteregger, Solar Extreme Ultraviolet Photon Flux Measurements in the Upper Atmosphere of August 1961, paper presented at 5th COSPAR Meeting May 1962, Washington, D.C.

29. Detweiler, C. R., D. L. Garrett, J. P. Purcell, and R. Tousey, The intensity distribution in the ultraviolet solar spectrum, Ann. Geophys. 17, 263 (1961).

30. Shklovskii, I. S., The ultraviolet radiation and X-rays of the sun, Soviet Physics Uspekhi 4, 812 (1962).

31. Ditchburn, R. W. and U. Őpik, Photoionization processes, in Atomic and Molecular Processes, edited by D. R. Bates. Academic Press, New York, 1962, p. 79.

32. Nicolet, M. and A. C. Aitken, The formation of the D-region of the ionosphere, J. Geophys. Res. 65, 1464 (1960).

AD Accession No.

STANFORD RESEARCH INSTITUTE, Menlo Park, California

IONIZATION IN AFTERBURNING ROCKET EXHAUSTS by Conrad F. Schadt, January 1963, 35 pp. 5 Figs.

(Project PAU-4134-1) Quarterly Report No. 2, Part I; AF SSD-TDR-63-42 [Contract AF 04(694)-128] Unclassified Report

Calculations have been made of "flame" (or mixing) dimensions associated with afterburning in rocket exhaust at high altitudes for a hypothetical rocket and trajectory. From these and a given exhaust composition one can estimate concentrations and times available for reactions of interest. Above some altitudes if observed flame lengths should turn out to be much greater, it would indicate that reaction rates rather than mixing rates were controlling.

Investigation of negative ion formation reactions indicates that they may not be a significant

UNCLASSIFIED

1. Exhaust gases—Ionization
2. Flames—Ionization
3. Exhaust gases—Motion
4. Jet Mixing Flow

I Schadt, Conrad F.

II Air Force Space Systems Division

III Contract AF 04(694)-128

AD Accession No.

STANFORD RESEARCH INSTITUTE, Menlo Park, California

IONIZATION IN AFTERBURNING ROCKET EXHAUSTS by Conrad F. Schadt, January 1963, 35 pp. 5 Figs.

(Project PAU-4134-1) Quarterly Report No. 2, Part I; AF SSD-TDR-63-42 [Contract AF 04(694)-128] Unclassified Report

Calculations have been made of "flame" (or mixing) dimensions associated with afterburning in rocket exhaust at high altitudes for a hypothetical rocket and trajectory. From these and a given exhaust composition one can estimate concentrations and times available for reactions of interest. Above some altitudes if observed flame lengths should turn out to be much greater, it would indicate that reaction rates rather than mixing rates were controlling.

Investigation of negative ion formation reactions indicates that they may not be a significant

UNCLASSIFIED

1. Exhaust gases—Ionization
2. Flames—Ionization
3. Exhaust gases—Motion
4. Jet Mixing Flow

I Schadt, Conrad F.

II Air Force Space Systems Division

III Contract AF 04(694)-128

factor in removal of electrons, since dissociative recombination of polyatomic ions is much faster. However, if the production of electrons were mainly due to ionization of alkali metals (which have very low recombination coefficients), the above reactions could be an important electron-removal mechanism. Calculations have been made of electron densities resulting from thermal ionization of potassium in a rocket engine at various altitudes to provide estimates for comparison and evaluation of the probable significance of other reactions. The estimates indicate that thermal ionization of potassium with typical solid propellants can be a very important source of electrons. Preliminary investigation of photoionization in a rocket exhaust has provided some values of radiation flux density versus altitude for various wavelengths.	UNCLASSIFIED	factor in removal of electrons, since dissociative recombination of polyatomic ions is much faster. However, if the production of electrons were mainly due to ionization of alkali metals (which have very low recombination coefficients), the above reactions could be an important electron-removal mechanism. Calculations have been made of electron densities resulting from thermal ionization of potassium in a rocket engine at various altitudes to provide estimates for comparison and evaluation of the probable significance of other reactions. The estimates indicate that thermal ionization of potassium with typical solid propellants can be a very important source of electrons. Preliminary investigation of photoionization in a rocket exhaust has provided some values of radiation flux density versus altitude for various wavelengths.	UNCLASSIFIED
factor in removal of electrons, since dissociative recombination of polyatomic ions is much faster. However, if the production of electrons were mainly due to ionization of alkali metals (which have very low recombination coefficients), the above reactions could be an important electron-removal mechanism. Calculations have been made of electron densities resulting from thermal ionization of potassium in a rocket engine at various altitudes to provide estimates for comparison and evaluation of the probable significance of other reactions. The estimates indicate that thermal ionization of potassium with typical solid propellants can be a very important source of electrons. Preliminary investigation of photoionization in a rocket exhaust has provided some values of radiation flux density versus altitude for various wavelengths.	UNCLASSIFIED	factor in removal of electrons, since dissociative recombination of polyatomic ions is much faster. However, if the production of electrons were mainly due to ionization of alkali metals (which have very low recombination coefficients), the above reactions could be an important electron-removal mechanism. Calculations have been made of electron densities resulting from thermal ionization of potassium in a rocket engine at various altitudes to provide estimates for comparison and evaluation of the probable significance of other reactions. The estimates indicate that thermal ionization of potassium with typical solid propellants can be a very important source of electrons. Preliminary investigation of photoionization in a rocket exhaust has provided some values of radiation flux density versus altitude for various wavelengths.	UNCLASSIFIED

STANFORD
RESEARCH
INSTITUTE

MENLO PARK
CALIFORNIA

Regional Offices and Laboratories

Southern California Laboratories
820 Mission Street
South Pasadena, California

Washington Office
808 17th Street, N.W.
Washington 5, D.C.

New York Office
270 Park Avenue, Room 1770
New York 17, New York

Detroit Office
The Stevens Building
1025 East Maple Road
Birmingham, Michigan

European Office
Pelikanstrasse 37
Zurich 1, Switzerland

Japan Office
911 Iino Building
22, 2-chome, Uchisaiwai-cho, Chiyoda-ku
Tokyo, Japan

Representatives

Honolulu, Hawaii
Finance Factors Building
195 South King Street
Honolulu, Hawaii

London, England
19 Upper Brook Street
London, W. 1, England

Milan, Italy
Via Macedonio Melloni 40
Milano, Italy

London, Ontario, Canada
P.O. Box 782
London, Ontario, Canada